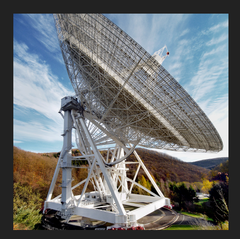

100-m Effelsberg
Located in Effelsberg it covers the band 2.64 - 43 GHz with a precision of a few percent for monthly sampling of 60 sources

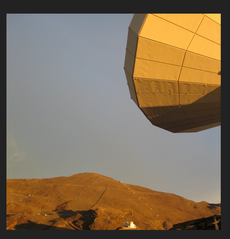

30-m IRAM
Located in Granada, Spain it covers the band 86 - 250 GHz monthly also for roughly 60 sources

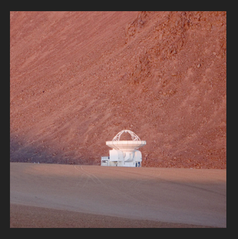

12-m APEX
It covers the 345 GHz band and it is located in Atacama desert in Chile at an altitude of 5100 m

the F-GAMMA program:
on the unification of continuum radio spectra variability patterns seen in *Fermi*-GST blazars

E. Angelakis, L. Fuhrmann, I. Nestoras, C. M. Fromm, J. A. Zensus, N. Marchili, T. P. Krichbaum, R. Schmidt (Max-Planck-Institut fur Radioastronomie, Bonn, Germany)
M. Perucho-Pla (Departament d'Astronomia i Astrof´ısica. Universitat de Valencia, Valencia, Spain)
H. Ungerechts, A. Sievers, D. Riquelme (Instituto de Radio Astronoma Milimétrica, Granada, Spain)
A. C. S. Readhead, V. Pavlidou, J. Richards, W. Max-Moerberck, T. Pearson (California Institute of Technology, Pasadena, USA)

Abstract

On the basis of Effelsberg and IRAM data alone (2.6 - 240 GHz), the broad-band spectra exhibit variability patterns which at first look appear erratic. As we discuss here, the apparent "ocean" of variability patterns (see **Figure 2**) can organized into **only 5 classes** on the basis of their phenomenological characteristics. Consequently, we propose that **4** of these classes can naturally be explained by the same principal system of a quiescent spectrum underlying a flaring event while for the last class an dependent mechanisms must be responsible.

The F-GAMMA program

The F-GAMMA program aims at understanding the physics at work in AGN via a multi-frequency monitoring approach. A number of roughly **65 *Fermi*-GST detectable blazars** are being **monitored monthly since January 2007** chiefly at radio wavelengths. The core program relies on the **100-m Effelsberg telescope** operating at 8 frequencies between 2.6 and 43 GHz, the **30-m IRAM** telescope observing at 86, 145 and 240 GHz and the **APEX 12-m** telescope at 345 GHz. Beyond that, the **OVRO 40-m telescope** team is approaching the problem in a complementary manner monitoring roughly 1200 sources a couple of times per week. Optical data are provided by the Abastomani 70-cm and 1.25-m telescopes.

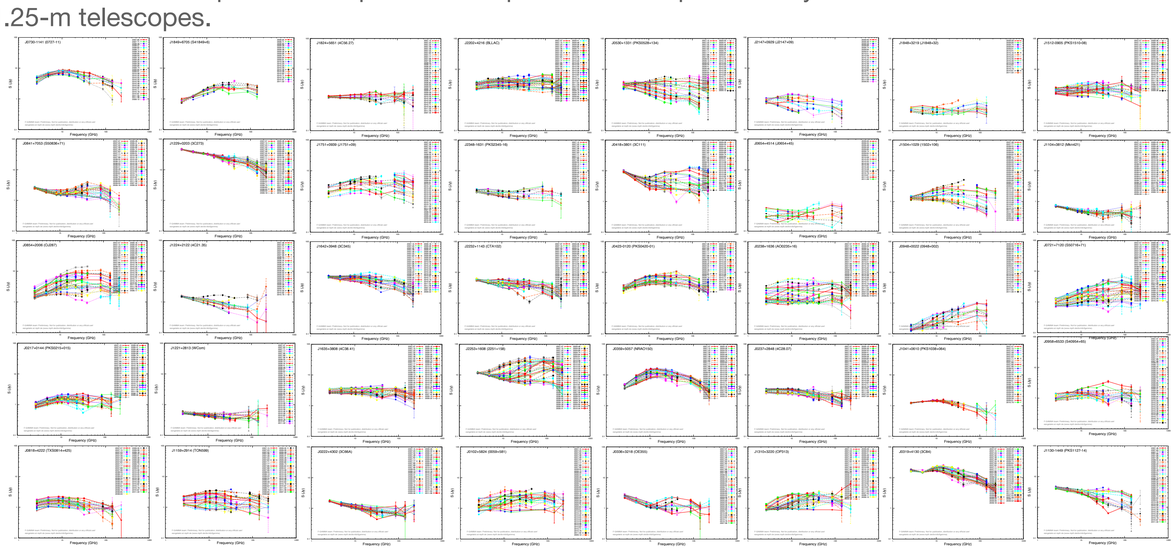

Figure 2

Examples of monthly sampled, broad-band radio spectra. Here Effelsberg and IRAM data alone are presented (2.6-240 GHz). The pluralism of variability patterns is apparent.

Phenomenological classification of the spectrum variability pattern

The variability patterns shown by any source in **Figure 2** can be classified in only one of **5 major "classes"** which are termed numerically between 1 and 5. (Four of them show also sub-classes):

A. "chromatic" classes:

Class 1 - Fig. 1(a): The variability pattern dominated by spectral evolution. The spectrum appears convex, its peak is drifting within the band-pass. The shape is changing to flat or mildly steep power law followed by new events. No evidence of quiescence spectrum.

Class 1b - Fig. 1(b): It shows same characteristics but the lowest frequency does not show significant variability. The activity seizes before this part of the spectrum but the flux density level reached is high compared to that at the lowest frequency.

Class 2 - Fig. 1(c): Also dominated by spectral evolution. The important difference is that the flux density at lowest frequency during the steepest spectrum phase is higher than that during the inverted spectrum phase. The maximum flux density reached is significantly above that at the lowest frequency. Hints that the observed steep spectrum is not a quiescence spectrum but the "echo" of a recent, outburst.

Class 3 - Fig. 1(d): Also dominated by the spectral evolution. The identifying characteristics is: (a) that the lowest frequency practically does not vary and, (b) the maximum flux density reached by outbursts is comparable to that at the lowest band-pass frequency. This leaves hints that the events seize very close to the lowest frequency of the band-pass and hence a quiescence spectrum is becoming barely evident.

Class 3b - Fig.1(e): Here however the quiescence spectrum is seen clearly at least at the 2 lowest frequencies.

Class 4 - Fig. 1(f): Sources of this type spend most of the time as steep spectrum ones which are sometimes showing an outburst of relatively low power propagating towards low frequencies.

Class 4b - Fig. 1(g): This type includes persistently steep spectrum cases.

B. "achromatic" classes:

Class 5 - Fig. 1(h): In this case the spectrum is convex and follows an "achromatic" evolution. That is, it shifts its position in the S – ν space preserving its shape.

Class 5b - Fig. 1(i): This type shows principal characteristics similar to the previous one but there is a significant shift of the peak (S_m, ν_m) towards lower frequencies as the peak flux density increases.

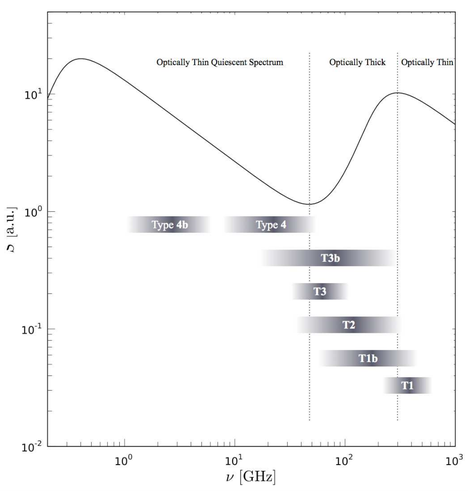

Figure 3

The 2-component principal system assumed to explain the observed phenomenologies for classes between 1 and 4b. The shaded area marks the observing band-pass.

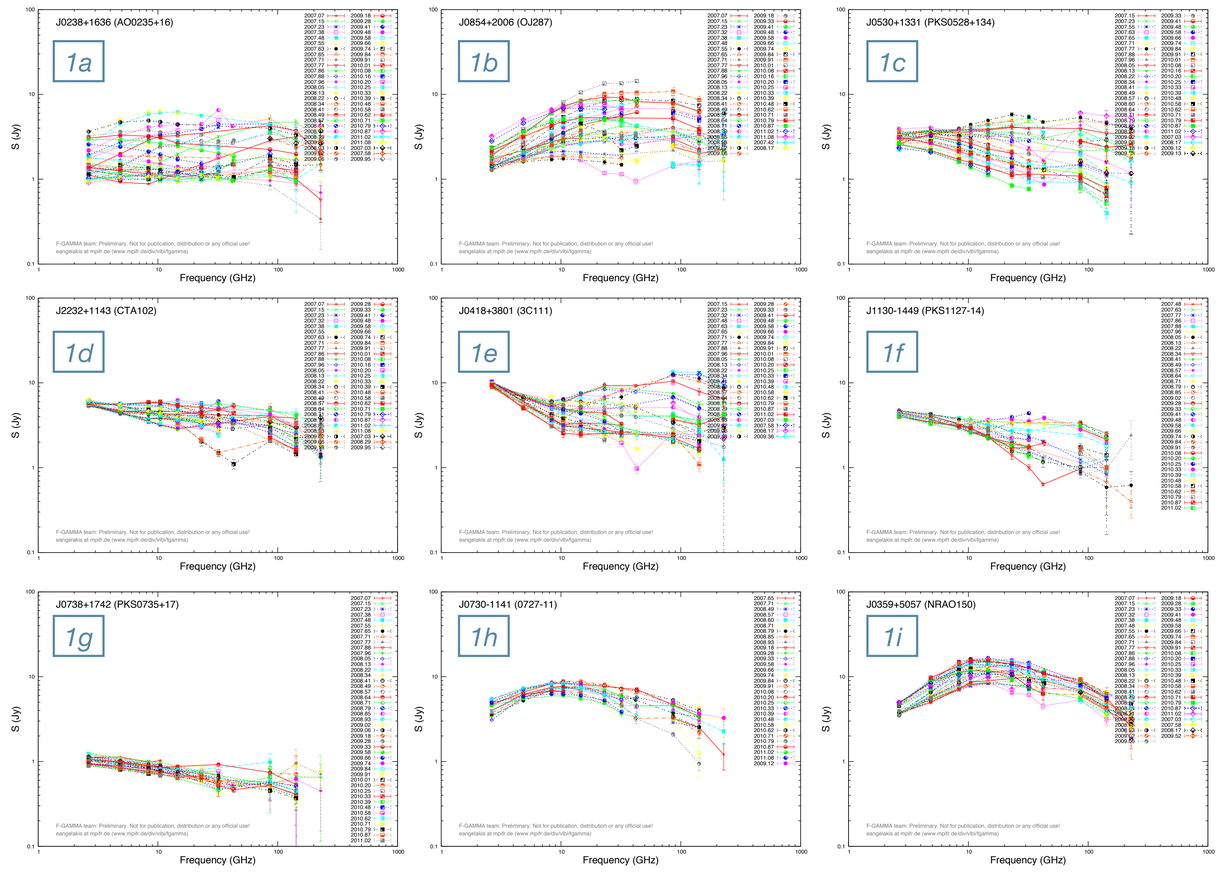

Figure 1

The prototypes for the 5 classes of our classification

Unification scheme for the variability patterns

All variability patterns from class 1 to 4b can all be naturally explained on the basis of a **two-component principal system** made of:

1. A **power law quiescence spectrum** with $S \sim \nu^{\alpha}$ (optically thin emission from relaxed large scale jet).
2. A **convex SSA spectrum** of an outburst superimposed on the quiescence part.

Figure 3 on the left captures the idea. The shaded areas denote our band-pass. On this ground the phenomenologies from class 1 to 4b are due to different:

1. **relative position** of the centre of our band-pass with respect to the source spectrum.
2. The **relative width** of the shaded areas relative to the width of the bridge (the total minimum) between the optically thick part of the outburst and the steep part of the quiescence spectrum denoting the fraction of the spectrum that the bandpass can sample.

Now the relative position and width of our band-pass with respect to the source spectrum can be modified from source-to-source by: (a) the **redshift** modulus and (b) **intrinsic properties** modulus.

Reproducing the observed phenomenologies

We assume that all the events are due to same process, (shocks evolving in jets), seen at different evolutionary stages nd different redshifts. We have then traced their temporal evolution using the shock-in-jet model (Marscher & Gear 1985; Tuerler et al. 2000). We have assumed three cases: 1. **weak source** with a **low quiescent spectrum**, 2. **medium source** with a **regular quiescent** spectrum, and 3. **powerful source** with a **high quiescent** spectrum. Then we follow its evolution:

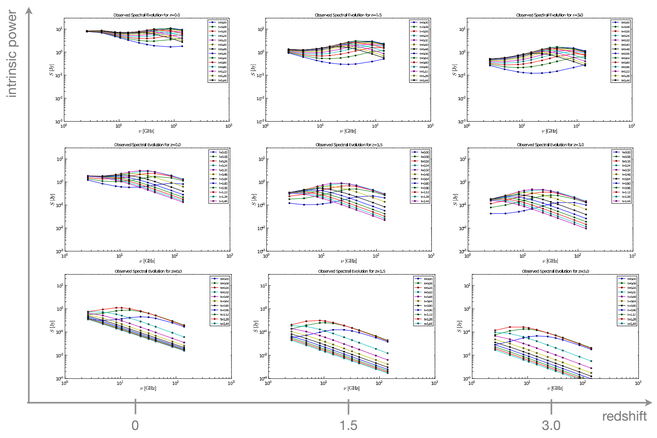

Conclusions

It appears that only two major mechanisms producing variability:

1. Spectral evolution dominated (chromatic)
2. achromatic variability mechanism

So far no source has shown a switch in type suggesting:
1.Either the mechanism is a source fingerprint
2.It is determined by source intrinsic properties that stay invariant in time or change with pace much slower than we can sample.

Although phenomenologies from 1-4b can well be explained by the shock-in-jet model, classes 5 and 5b are yet to investigated. Other mechanisms must be invented.

References

Marscher, A. P. & Gear, W. K. 1985, ApJ, 298, 114
Tuërler, M., Courvoisier, T., & Paltani, S. 2000, A&A, 361, 850

E. Angelakis, eangelakis@mpifr.de

For more information please visit:
www.mpifr.de/div/vlbi/fgamma